Traffic Performance and Mobility Modeling of Cellular Communications with Mixed Platforms and Highly Variable Mobilities

PHILIP V. ORLIK, STUDENT MEMBER, IEEE, AND STEPHEN S. RAPPAPORT, FELLOW, IEEE

In modeling teletraffic performance of mobile cellular networks, previous work has made use of the concept of dwell time—a random variable that describes the amount of time a platform remains in a cell, sector, or microcell. The dwell time was characterized as a negative exponential variate or the sum of negative exponential variates. With a suitable state description, this allows use of the memoryless property of negative exponential variates with the result that the problem of computing traffic performance characteristics can be cast in an underlying framework based on multidimensional birth-death processes. Many alternative system configurations and issues can be investigated using this approach. In small cell (microcellular) systems, however, cell sizes tend to be much less regular in shape and size, and differences in paths traversed by mobiles have a large impact on dwell-time realizations. Succinctly, some mobile platform classes have mobility characteristics that are highly variable, in that dwell-time standard deviation is greater than the mean. The previous models, in which dwell time is a negative exponential or sum of exponential variates, may not be adequate in such cases because they can only accommodate dwell-time variates for which the standard deviation does not exceed the mean. We seek to extend the analytical framework so that highly variable mobilities can be considered while insights, tools, approaches, and formulations that are facilitated by the framework can be exploited. The approach allows computation of major teletraffic performance characteristics for cellular communications in which mobility issues are important. In this paper, we consider multiple platform types as well as cutoff priority for handoffs. Additional issues can be considered using this same approach. Computational issues are discussed, and some theoretical performance characteristics are obtained to demonstrate the method and compare with previous work.

Keywords— *Cellular communications, communications traffic performance, mobility modeling.*

I. INTRODUCTION

Cellular systems must deliver a variety of services to many types of users having a wide range of mobility characteristics. The envisioned systems and the services they will provide (voice, data, e-mail, etc.) are sometimes difficult to model. Much of the difficulty in developing analytically tractable models arises from the mobility of the network users, especially the handoffs required by such users. The effects of user mobility on system performance are a central issue for the design and implementation of mobile networks.

The development of analytically tractable models to compute teletraffic performance characteristics of mobile wireless networks has been the thrust of recent work [1]–[6]. A family of models that is widely applicable is based on multidimensional birth-death processes [7]. An essential feature is the characterization of platform mobility by a *dwell time*. The dwell time of a platform is defined as a random variable that gives the amount of time that a platform can maintain a satisfactory two-way communication link with a given network gateway. A platform's dwell time depends on many factors, including speed, path, transmitting power, signal propagation, and interference. References [2], and [8]–[10] discuss performance measures that are important for cellular systems. Mobility models are necessary for the analysis of many additional pertinent cellular issues. Some of these include signaling load associated user location [11]–[13] and handoff initiation algorithms [14]–[16].

When analytical models are desired, simple descriptions of user movement are sometimes used. These have included negative exponential distributed (NED) dwell times, as reported in [1], [2], [3], [17], and [18], or a sum of negative exponential random variables, as in [2]. Such mobility models allow for the analytical computation of performance characteristics, as described in [7]. This paper extends earlier work [2] to include a class of dwell-time probability density functions (pdf's) with coefficients of variation greater than one.

The coefficient of variation (denoted here by κ) of a random variable (RV) is defined as the ratio of its standard deviation to its mean. This is a common measure of the

Manuscript received June 10, 1997; revised January 21, 1998. This work was supported in part by the U.S. National Science Foundation under Grant NCR 94-15530 and in part by BMDO/IST under Grant N00014-9511217 administered by the Office of Naval Research.

The authors are with the Department of Electrical Engineering, State University of New York at Stony Brook, Stony Brook, NY 11794-2350 USA (e-mail: porlik@sbee.sunysb.edu; rappaport@sbee.sunysb.edu).

Publisher Item Identifier S 0018-9219(98)04244-3.

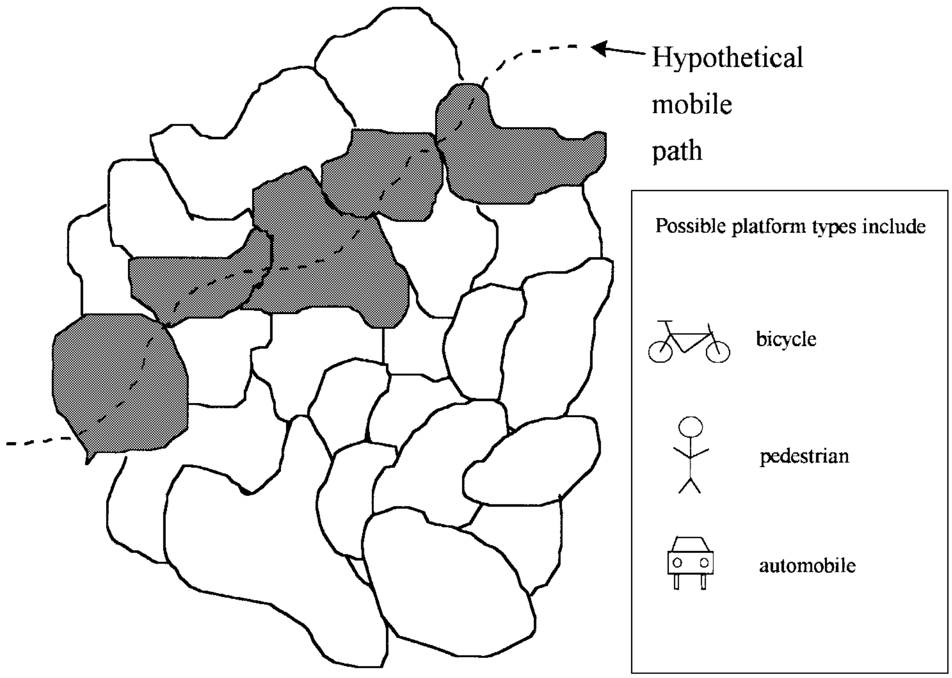

Fig. 1. Microcellular system with multiple platform types.

random variable's dispersion about its mean. Previous work modeled the platform dwell time as the sum of statistically independent negative exponential random variables. This approach results in a dwell-time RV with $\kappa \leq 1$ (with equality when there is only one term in the sum). In the case of macrocellular systems, cell sizes are relatively large compared with shape, size, and path variations. A dwell-time variate with a coefficient of variation of one or less seems to be a reasonable model for platform mobility. For microcellular systems, however, such dwell-time variates have less intuitive appeal.

Microcellular systems have small cells, which lead to smaller mean dwell times for platforms traversing the system (at the same speeds). Also, since the transmitting power is reduced, obstacles such as buildings, trees, hills, etc. will have a greater effect on cell size and shape. The result is that cells in a microcellular system tend to be less regular in shape and more variable throughout the coverage area. This large variation in cell size and shape, together with the shorter mean dwell time, suggests consideration of dwell-time variates with coefficients of variation that are greater than one. Fig. 1 illustrates the irregularity of cell shape in a microcellular system and also the presence of a variety of platform types in the system.

The motivation here is to develop a more complete framework in which theoretical performance measures can be calculated for dwell-time variates having arbitrary coefficients of variation. Then, an appropriate pdf for the dwell time can be chosen from a family of models, and its parameters can be adjusted to fit empirical data. For example, if data show that dwell times are highly concentrated around a mean value, then a pdf with $\kappa < 1$ would be a suitable choice for a dwell-time model. On the other hand, if dwell times are found to be widely dispersed, then a more realistic pdf with $\kappa > 1$ could be used as a dwell-time model. The multidimensional birth-death framework and approach to the problem is expounded in [7] and has already been extended to consider various system issues. These include platforms that can support multiple calls simultaneously [1], systems with multiple platform types with different mobility characteristics [2], mixed platform mobilities, and a variety of services requiring a multiplicity of resources present in the same system [5]. In [5], loss- and delay-type queueing methods were also considered. Nonhomogeneous systems with imperfect handoff initiation are considered in [2]. Hierarchically overlaid systems [6], overlapping coverage areas [19], and soft handoff [20] have also been accommodated within the same framework. The current paper extends the framework to a wider range of dwell-time models.

Other approaches to mobility modeling have been investigated. Rather than assume a pdf for the dwell time, a study reported in [21] traced mobile paths in an environment where movement is governed by a set of random variables. There, it was reported that a Gamma distribution can describe mobile dwell times. The Gamma distribution can be used to model dwell-time variates with large coefficients of variation; however, it does not have the required memoryless property and cannot be used in the multidimensional birth-death framework. Some other studies model mobility as a random walk [22]. An extension of this to characterizing user movement as a diffusion process is given in [23]. An overview of other mobility modeling techniques is given in [24]. These include fluid models, random walks, gravity models, and mobility traces. These modeling techniques do not generally fit into the framework we are proposing and will not be discussed further. One other relevant and recent study is reported in [25], where the authors have simulated a cellular communication network using a variety of pdf's as dwell-time models.

In this paper, we model the dwell time as a sum of statistically independent random variables, each distributed according to a hyperexponential pdf. The hyperexponential has been used in queueing theory to model service times that have large coefficients of variation [26]. As discussed in Section III, the hyperexponential alone is not intuitively satisfying as a dwell-time model because of the behavior of the pdf near the origin. We have therefore generalized to a sum of independent hyperexponential variates. With a proper state description, this approach allows the memoryless property to be used. The framework to compute traffic-performance measures for a cellular system with platforms having such mobility characteristics is developed. Theoretical traffic-performance characteristics are calculated for various values of κ (less than, equal to, greater than unity). Results are compared. The discussion is presented for systems that have *mixed* platform types. That is, platforms having different mobility characteristics are present in the system at the same time.

II. Model Description

The system description given here is similar to that of [2]. We consider a large geographical region covered by cells. Mobile platforms traverse the region and can each support a maximum of one call. We assume that in each cell, there is one gateway with C channels assigned to it. A cutoff priority scheme is used so that C_h channels in each cell are reserved for handoff calls. Specific channels are not reserved, just a fixed number. That is, new calls that arise in a cell will not be served if there are fewer than C_h idle channels.

We allow for multiple platform *types*, which are indexed by $g = 1, 2, \cdots, G$. Each platform type has distinct mobility characteristics. These are characterized by the statistical properties of the dwell time of a platform of the given type. The dwell time of a platform of type g is a random variable denoted by $T_D(g)$. At each gateway, there may also be quotas assigned so that no more than $J(g)$ channels can be occupied by calls on g-type platforms at the same time. In this paper, it is assumed that the system is *homogeneous* and that handoff detection and initiation is *perfect*. Therefore, all *valid* handoff needs are detected, and no unnecessary handoff initiations are generated. Relaxation of these assumptions can be accommodated within the same framework [2].

III. Probability Distributions for Dwell Times

A. Sum of Negative Exponentials

The first distribution we discuss results from summing independent negative exponential random variables. This was used to characterize dwell time in [2]. The random variable $T_D(g)$ is the sum of $N(g)$ statistically independent random variables denoted $T_D(g,i)$, $i = 1, 2, 3, \cdots, N(g)$ in which $T_D(g,i)$ has a negative exponential pdf with mean $\bar{T}_D(g,i) = 1/\mu_D(g,i)$ and variance $\mathrm{VAR}[T_D(g,i)] = 1/[\mu_D(g,i)]^2$. We define $N(g)$ as the number of dwell-time phases for a platform of type g [2]. The mean and variance of $T_D(g)$ can be written as

$$\bar{T}_D(g) = \sum_{i=1}^{N(g)} \bar{T}_D(g,i) = \sum_{i=1}^{N(g)} \frac{1}{[\mu_D(g,i)]} \tag{1}$$

and

$$\mathrm{VAR}[T_D(g)] = \sum_{i=1}^{N(g)} 1/[\mu_D(g,i)]^2. \tag{2}$$

The squared coefficient of variation (κ^2) is given by

$$\kappa^2[T_D(g)] = \frac{\mathrm{VAR}[T_D(g)]}{[\bar{T}_D(g)]^2} = \frac{\sum_{i=1}^{N(g)} 1/[\mu_D(g,i)]^2}{\left[\sum_{i=1}^{N(g)} 1/\mu_D(g,i)\right]^2}. \tag{3}$$

Expanding the denominator in (3), we can obtain

$$\kappa^2[T_D(g)] = \frac{\sum_{i=1}^{N(g)} 1/[\mu_D(g,i)]^2}{\sum_{i=1}^{N(g)} 1/[\mu_D(g,i)]^2 + \text{other nonnegative terms.}} \tag{4}$$

Since all the terms on the right side of (4) are nonnegative, we have the result that $\kappa^2[T_D(g)]$ must be less than or equal to one. This result holds for any dwell-time variate that is constructed using a sum of statistically independent NED variates.

This formulation of the dwell time leads to an analytically tractable model. Although strictly, the individual dwell-time components $T_D(g,i)$ do not have any direct physical meaning, conceptually, one can suppose that a platform of type g enters a cell and completes $N(g)$ *phases* of dwell time. Completion of the last dwell-time phase corresponds to leaving the cell (the completion of dwell time) [2]. If all $N(g)$ phases of dwell time are identically distributed, that is, $\mu_D(g,i) = \mu_D$ for $i = 1, 2, \cdots, N(g)$, we have the special case of the Erlang distribution. The squared coefficient of variation reduces to $\kappa^2[T_D(g)] = 1/N(g)$ [2].

Fig. 2 is a plot of the Erlang distribution for $N(g) = 1, 2, 3, 4$ and $\bar{T}_D(g) = 1$. The reader will note that when the number of phases is one $(N(g) = 1)$, the Erlang distribution reduces to the NED with $\kappa = 1$. Increasing $N(g)$ causes κ to decrease. The respective squared coefficient of variations are $\kappa^2 = 1, 1/2, 1/3, 1/4$. The figure shows that as the number of phases $[N(g)]$ increases, the pdf becomes more concentrated around its mean. A state characterization and a method to compute performance measures are given in [2].

B. Hyperexponential

The hyperexponential pdf is a weighted sum of exponential functions. The pdf has the form

$$f_{T_D}(t) = \sum_{k=1}^{M} \alpha(k) \cdot \mu_D(k) \cdot \exp(-\mu_D(k) \cdot t) \tag{5}$$

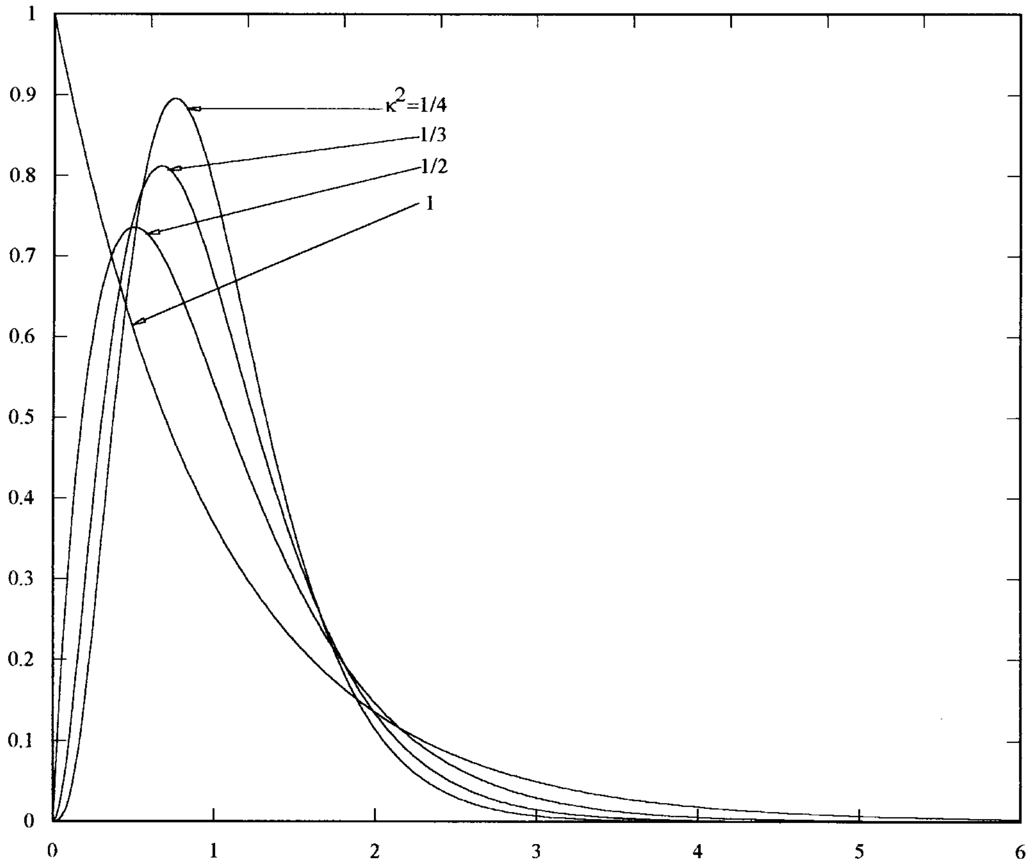

Fig. 2. Erlang pdf's with mean $= 1$ and $\kappa^2 = 1, 1/2, 1/3, 1/4$.

where

$$\sum_{k=1}^{M} \alpha(k) = 1 \quad \text{and} \quad \alpha(k) > 0. \tag{6}$$

Equation (5) represents an M *stage* hyperexponential pdf, where $k = 1, 2, \cdots, M$. One can suppose that the pdf (5) is that of a random variable generated in the following way. Choose a negative exponential random variable from a set of M possibilities. The probability of choosing the kth NED random variable is given by the parameter $\alpha(k)$ $(k = 1, 2, \cdots, M)$. The value of the random variable T_D is then a realization of the chosen NED random variable.

The mean of the hyperexponential is

$$\bar{T}_D = \sum_{k=1}^{M} \frac{\alpha(k)}{\mu_D(k)} \tag{7}$$

The variance, σ^2_{HYP}, of the M stage hyperexponential is given by

$$\sigma^2_{\mathrm{HYP}} = \left[\sum_{k=1}^{M} \frac{2 \cdot \alpha(k)}{[\mu_D(k)]^2}\right] - \left(\bar{T}_D\right)^2. \tag{8}$$

We can write the squared coefficient of variation as

$$\kappa^2 = \frac{\sigma^2_{\mathrm{HYP}}}{(\bar{T}_D)^2} = \frac{2 \cdot \left[\sum_{k=1}^{M} \frac{\alpha(k)}{[\mu_D(k)]^2}\right] - \left(\bar{T}_D\right)^2}{(\bar{T}_D)^2}. \tag{9}$$

The sum in (9) can be thought of as the expectation of X^2, $(E[X^2])$, where X is a discrete random variable X that takes on values $\{1/\mu_D(1), 1/\mu_2(2), \cdots, 1/\mu_D(k), \cdots, 1/\mu_D(M)\}$ with respective probability of occurrence $\alpha(k)$. Since the variance $(\mathrm{VAR}[X] = E[X^2] - \{E[X]\}^2 \geq 0)$ of any random variable is nonnegative, we have $E[X^2] \geq \{E[X]\}^2$. We note that $E[X]$ is identical to $(\bar{T}_D)$ in (7). The substitutions yield

$$\begin{aligned} \kappa^2 &= \frac{2 \cdot \left[\sum_{k=1}^{M} \frac{\alpha(k)}{[\mu_D(k)]^2}\right] - (\bar{T}_D)^2}{(\bar{T}_D)^2} \\ &\geq \frac{2 \cdot \left[\sum_{k=1}^{M} \frac{\alpha(k)}{\mu_D(k)}\right]^2 - (\bar{T}_D)^2}{(\bar{T}_D)^2} \\ &= \frac{2 \cdot (\bar{T}_D)^2 - (\bar{T}_D)^2}{(\bar{T}_D)^2} = 1. \end{aligned} \tag{10}$$

Thus, the coefficient of variation for a hyperexponential RV is greater than or equal to one.

A state characterization can be given that allows multidimensional birth-death processes to be used to determine the state probabilities for a system with platform dwell times distributed according to the M stage hyperexponential pdf. One can conceptualize a platform that traverses the system. Each time the platform enters a new cell, it chooses a stage from the M stages available for its dwell time in the new cell. The kth stage is chosen with probability $\alpha(k)$. Upon completion of this stage, the platform will enter another

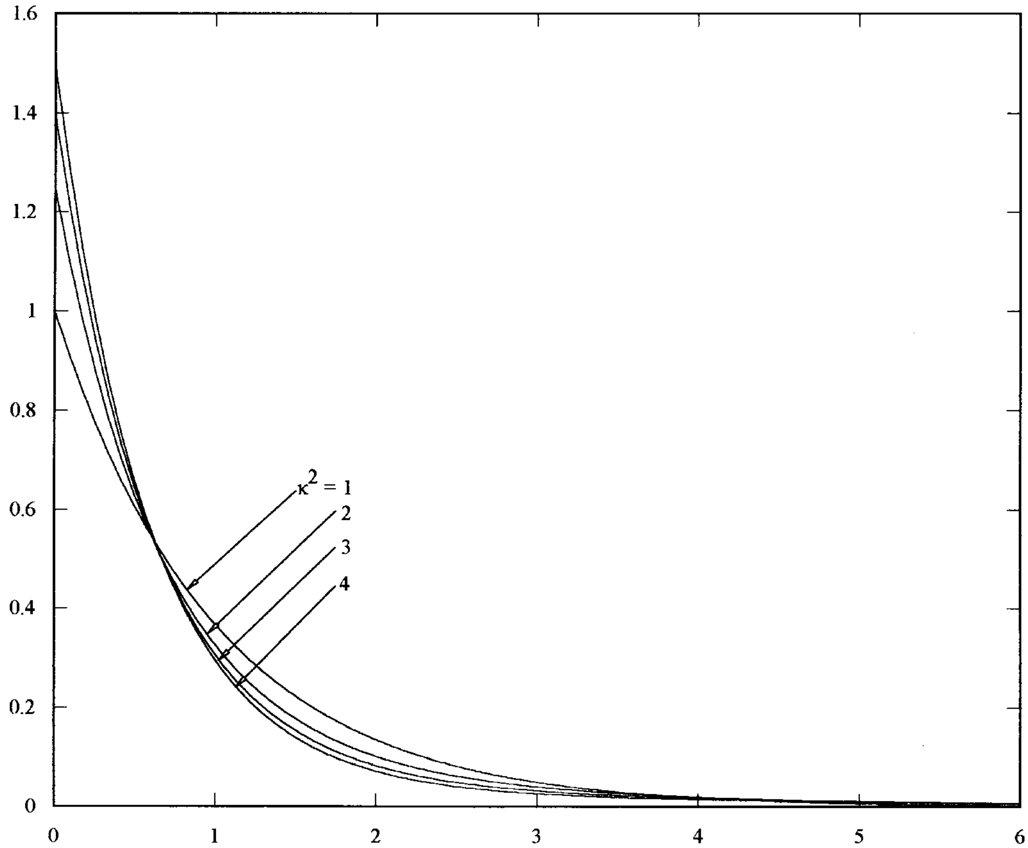

Fig. 3. Hyperexponential pdf's with mean $= 1$ and $\kappa^2 = 1, 2, 3, 4$.

cell, where it will again choose a new stage. It is important for the reader to notice the difference between the terms *phases* and *stages*.

If we set M equal to two, the result is a two-stage hyperexponential pdf. The variance of the two-stage exponential can be expressed as

$$\sigma^2_{\mathrm{HYP}} = \frac{2\alpha(1) - \alpha^2(1)}{\mu_D(1)^2} + \frac{2\alpha(2) - \alpha^2(2)}{\mu_D(2)^2} - \frac{2\alpha(1) \cdot \alpha(2)}{\mu_D(1) \cdot \mu_D(2)}. \tag{11}$$

With appropriate choices of $\alpha(1)$, $\alpha(2)$, $\mu_D(1)$, and $\mu_D(2)$, the coefficient of variation for the hyperexponential pdf can be set at any value greater than one. Fig. 3 is a plot of several hyperexponential functions for $\kappa^2 = 1, 2, 3, 4$ and mean equal to one. However, the hyperexponential's behavior near zero is intuitively unsatisfying for a dwell-time model. This is because the pdf is nonzero at the origin and may have too much of its weight below its mean. This has the effect of giving *extremely* short dwell times a high probability of occurrence. In addition, this low weighting near the origin will increase as κ increases. Extremely short dwell times are possible in microcellular systems but not to the extent that the hyperexponential favors them.

C. Sum of Hyperexponentials (SOHYP)

We seek a dwell-time pdf $f_{T_D(g)}(t)$, which has the following properties: $\kappa > 1$, $f_{T_D(g)}(0) = 0$; and which allows analytically tractable models to be constructed within the multidimensional birth-death process framework. For this purpose, consider a sum of statistically independent hyperexponential variates. The resulting pdf we call the SOHYP. With the appropriate choice of parameters, the corresponding random variable distributed according to this pdf can have a coefficient of variation greater than one. In the special case for which each hyperexponential in the sum has only a single stage, the resulting variate is a sum of exponential variates—which, according to (4), has a coefficient of variation that is less than one. Thus, the SOHYP is a pdf that provides a generalization in this regard and (as we shall see) allows use of the multidimensional birth-death framework.

The dwell time for a g-type platform is a random variable $T_D(g)$. $T_D(g)$ is defined to be the sum of $N(g)$ statistically independent, hyperexponentially distributed random variables denoted $T_D(g,i)$, where $i = 1, 2, \cdots, N(g)$. We again will make use of the concept of *phases*. Each random variable $T_D(g,i)$ is considered a phase of $T_D(g)$, and each phase can have any number of *stages* indexed by $k = 1, 2, \cdots, M(g,i)$. $M(g,i)$ is the number of stages for a g-type platform in the ith phase. From (7), we can find the mean of $T_D(g)$

$$\bar{T}_D(g) = \sum_{i=1}^{N(g)} \sum_{k=1}^{M(g,i)} \frac{\alpha(g,i,k)}{\mu_D(g,i,k)}. \tag{12}$$

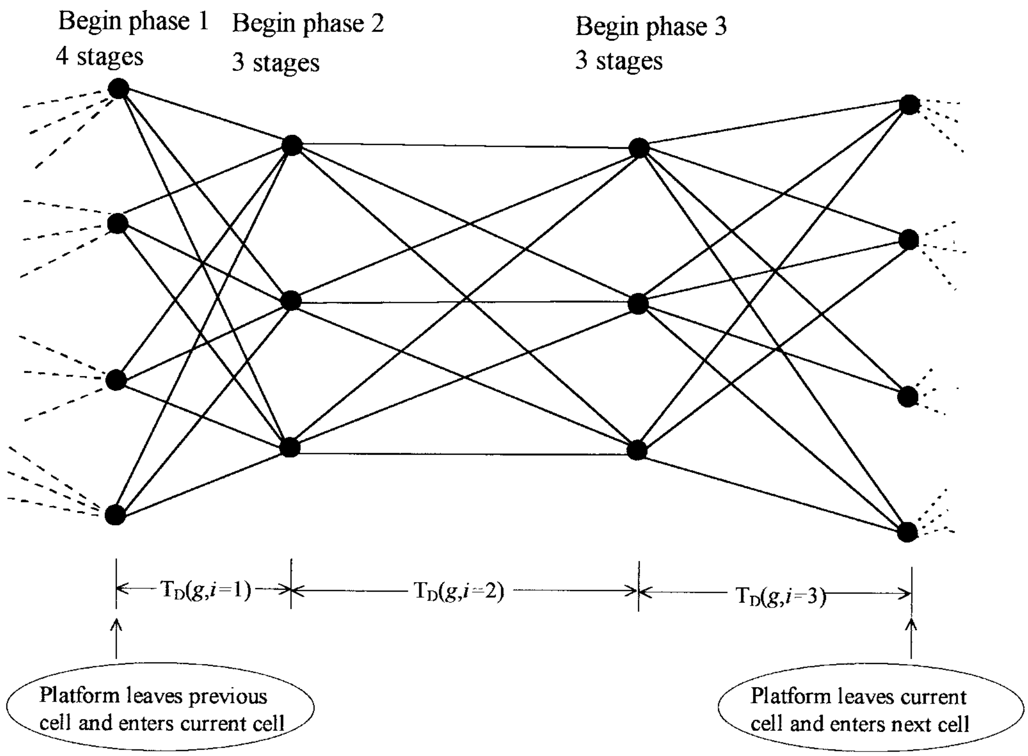

Fig. 4. Construction of SOHYP dwell times from hyperexponential phases. SOHYP with three phases: phase one, four-stage hyperexponential; phase two, three-stage hyperexponential; phase three, three-stage hyperexponential.

The variance VAR$[T_D(g)]$ is the sum of the variances of $T_D(g,i)$

$$\text{VAR}[T_D(g)] = \sum_{i=1}^{N(g)} \sigma^2_{\text{HYP}}(g,i). \tag{13}$$

Conceptually, one can suppose that a g-type platform traversing a cell completes a sequence of phases. When the platform enters a cell, it begins phase one of its dwell time. It chooses a dwell-time stage for this phase from the $M(g,1)$ stages available for phase one. The particular stage k is chosen with probability $\alpha(g,1,k)$. When the first phase is completed, the platform enters the second phase. It chooses a new dwell-time stage from the $M(g,2)$ stages available for the second phase. The choice of stage k is made with probability $\alpha(g,2,k)$. The choice of stage is independent from one phase to the next. This process continues until the platform enters its *final* phase, $i = N(g)$. Completion of this last phase represents the platform's exiting the cell (moving out of communication range of the base station).

Fig. 4 is a diagram of the above process shown for a three-phase SOHYP $(N(g) = 3)$, with four stages in its first phase $(M(g,1) = 4)$ and three stages in each of its two remaining phases $(M(g,2) = M(g,3) = 3)$. Each node in the figure corresponds to the negative exponential random variable associated with that particular phase and stage.

This approach to dwell-time modeling (using a sum of statistically independent random variables) has the desirable effect of forcing the pdf of the dwell-time variate $f_{T_D(g)}(t)$ to zero at origin. In fact, for an $N(g)$ phase SOHYP pdf, with $N(g) > 1$, we have $f_{T_D(g)}(0) \equiv 0$. In addition, for $N(g) > 2$, the first $N(g) - 2$ derivatives are zero at the origin. We show this by use of the Laplace transform and its initial value theorem [27]. $T_D(g)$ has been defined to be a sum of statistically independent hyperexponentially distributed random variables $[T_D(g,i)]$. From probability theory, we know that the pdf $f_{T_D(g)}(t)$ is the convolution of the component pdf's $f_{T_D(g,i)}(t)$ [28]. That is

$$f_{T_D(g)}(t) = f_{T_D(g,1)}(t) * f_{T_D(g,2)}(t) * \cdots * f_{T_D(g,N(g))}(t). \tag{14}$$

Let $\tilde{F}(\zeta)$ denote the Laplace transform of some function $f(t)$, in which ζ is the transform variable. Taking the Laplace transform of (14) and using (5), we find that $\tilde{F}_{T_D(g)}(\zeta)$ can be written in the form

$$\tilde{F}_{T_D(g)}(\zeta) = \prod_{i=1}^{N(g)} \sum_{k=1}^{M(g,i)} \frac{\alpha(g,i,k) \cdot \mu_D(g,i,k)}{\zeta + \mu_D(g,i,k)}. \tag{15}$$

We note that in general, $\tilde{F}_{T_D(g)}(\zeta)$ is a rational polynomial function of ζ, which has the form $\tilde{F}_{T_D(g)}(\zeta) = N(\zeta)/D(\zeta)$, where $N(\zeta)$ and $D(\zeta)$ are the numerator and denominator, respectively. From (15), we see that the degree of $N(\zeta)$ is 0 and the degree of $D(\zeta)$ is $N(g)$. Therefore, $\tilde{F}_{T_D(g)}(\zeta)$ is a strictly proper rational function (that is, the degree of the denominator is strictly greater than that of the numerator).

A useful property of the Laplace transform states that for positive time functions ($f(t) = 0$ for $t < 0$), the

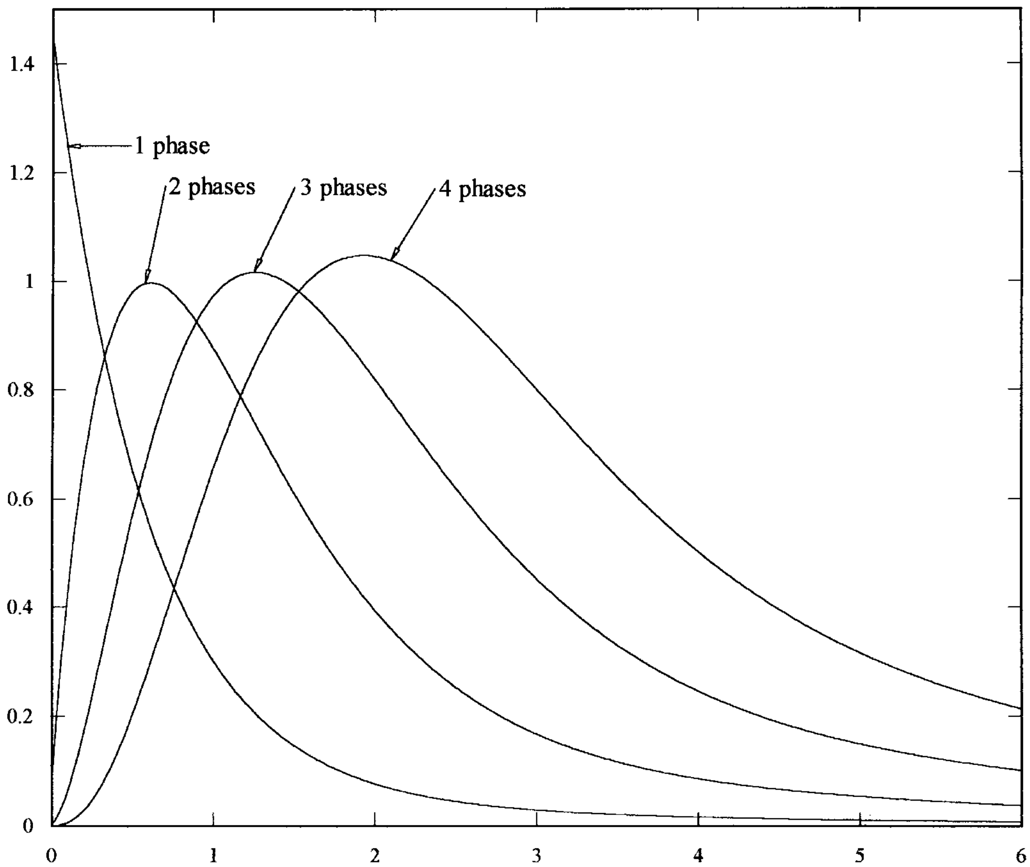

Fig. 5. SOHYP pdf for $N = 1, 2, 3, 4$.

transform of the jth derivative of $f(t)$ is $\zeta^j \tilde{F}(\zeta)$ [27]. That is, the transform of the jth derivative of $f(t)$ is simply the transform of $f(t)$ multiplied by ζ^j. Then, for $f_{T_D(g)}(t)$, we have

$$\frac{d^{(j)}}{dt^{(j)}} f_{T_D(g)}(t) = f_{T_D(g)}^{(j)}(t) \leftrightarrow \zeta^j \cdot \tilde{F}_{T_D(g)}(\zeta). \tag{16}$$

We can now write a general expression for the Laplace transform of the jth derivative of $f_{T_D(g)}(t)$ as

$$\tilde{F}_{T_D(g)}^{(j)}(\zeta) = \zeta^j \tilde{F}_{T_D(g)}(\zeta). \tag{17}$$

The initial value theorem [27] for the Laplace transform states that the value of $f(0)$ is given by the limit as ζ tends to infinity of $\zeta \tilde{F}(\zeta)$. Applying the initial value theorem to (17), we have

$$f_{T_D(g)}^{(j)}(0) = \lim_{\zeta \to \infty} \zeta \cdot \tilde{F}_{T_D(g)}^{(j)}(\zeta) = \lim_{\zeta \to \infty} \zeta^{j+1} \cdot \tilde{F}_{T_D(g)}(\zeta). \tag{18}$$

Recall that $\tilde{F}_{T_D(g)}(\zeta)$ is a strictly proper rational polynomial function with numerator of degree zero and denominator of degree $N(g)$. The limit in (18) will tend to zero as long as $\zeta^{j+1}\tilde{F}_{T_D(g)}(\zeta)$ is strictly proper. This is true for $j \leq N(g) - 2$. Therefore, the first $N(g) - 2$ derivatives of $f_{T_D(g)}(t)$ are zero at the origin. For an $N(g)$ phase SOHYP pdf, this is expressed by the following:

$$f_{T_D(g)}(0) = 0 \tag{19}$$

and

$$\frac{d^{(j)}}{dt^{(j)}} f_{T_D(g)}(0) = 0 \quad \text{for } j = 0, 1, 2, \cdots, N(g) - 2. \tag{20}$$

Fig. 5 is a plot of several SOHYP pdf's for $N(g) = 1, 2, 3, 4$, which demonstrates this behavior. Each of the curves was generated by convolving $N(g)$ identical two-stage hyperexponential functions (each having $\overline{T}_D(g) = 1$, $\kappa^2 = 3$).

Analytical expressions for the variance and other moments of an $N(g)$ phase SOHYP random variable can become extremely complex. However, the moment generating function ($\Phi_{\text{SOHYP}}(\zeta) \hat{=} E\{\exp(\zeta T_D(g))\}$) is easily obtained, and it is given below

$$\Phi_{\text{SOHYP}}(\zeta) = \prod_{i=1}^{N(g)} \sum_{k=1}^{M(g,i)} \frac{\alpha(g,i,k) \cdot \mu_D(g,i,k)}{\mu_D(g,i,k) - \zeta}. \tag{21}$$

The SOHYP's moments can be obtained from the above.

Although our formulation is general, for the numerical calculations presented in this paper, we have used (for each platform type g) a special form of SOHYP with two phases, ($N(g) = 2$). The first phase consists of a single stage ($M(g,1) = 1$), and the second phase is a two-stage hyperexponential ($M(g,2) = 2$). Thus, for numerical purposes, we consider the dwell time of a platform to be a random variable, which is the sum of a negative exponential variate and a two-stage hyperexponential variate.

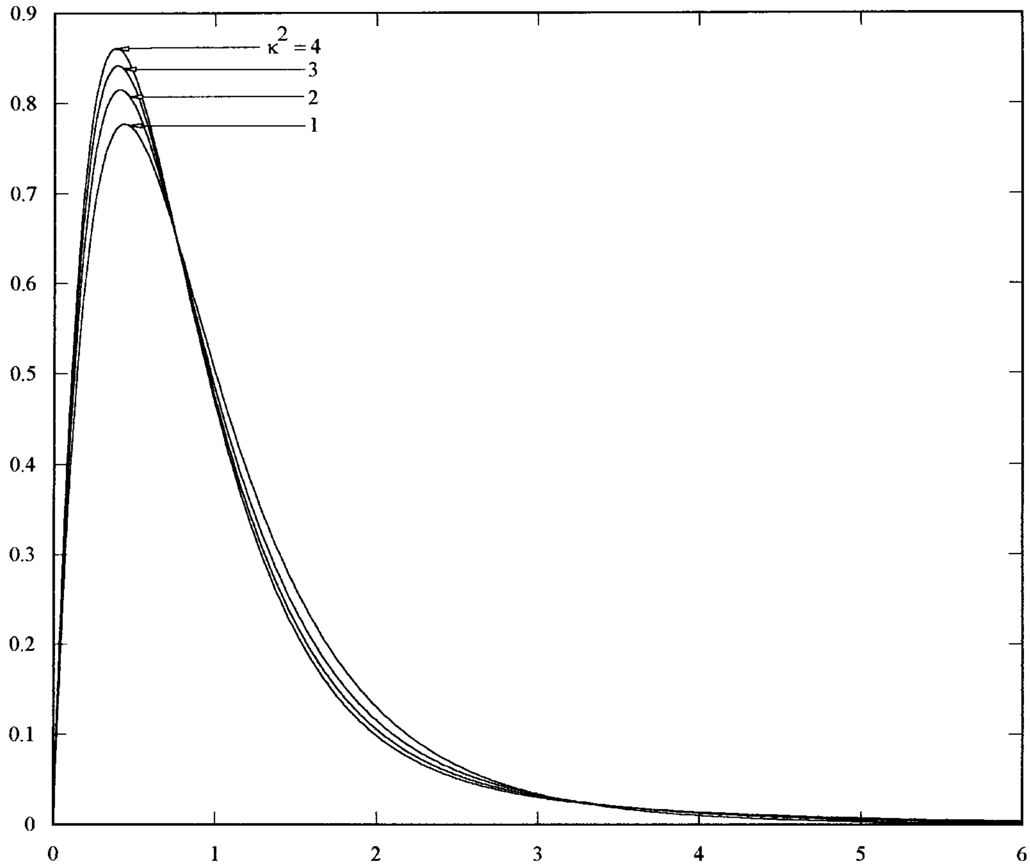

Fig. 6. Two-phase SOHYP pdf, phase one = negative exponential, phase two = two-stage hyperexponential. Mean = 1 and $\kappa^2 = 1, 2, 3, 4$.

If in addition we require that the μ_D parameter for the first phase be distinct from either μ_D parameter in the second phase, this special SOHYP pdf can be written as a weighted sum of exponentials. Specifically

$$\begin{aligned} f_{T_D(g)}(t) &= \left[\frac{\alpha(g,2,1)\cdot\mu_D(g,1,1)\cdot\mu_D(g,2,1)}{\mu_D(g,2,1)-\mu_D(g,1,1)}\right. \\ &\quad \left. + \frac{\alpha(g,2,2)\cdot\mu_D(g,1,1)\cdot\mu_D(g,2,2)}{\mu_D(g,2,2)-\mu_D(g,1,1)}\right] e^{-\mu_D(g,1,1)t} \\ &\quad + \left[\frac{\alpha(g,2,1)\cdot\mu_D(g,1,1)\cdot\mu_D(g,2,1)}{\mu_D(g,1,1)-\mu_D(g,2,1)}\right] e^{-\mu_D(g,2,1)t} \\ &\quad + \left[\frac{\alpha(g,2,2)\cdot\mu_D(g,1,1)\cdot\mu_D(g,2,2)}{\mu_D(g,1,1)-\mu_D(g,2,2)}\right] e^{-\mu_D(g,2,2)t} \end{aligned} \tag{22}$$

where $\mu_D(g,1,1) \neq \mu_D(g,2,1)$ and $\mu_D(g,1,1) \neq \mu_D(g,2,2)$.

While this special case allows four parameters that can be adjusted to fit empirical data for *each* platform type g, the specific form given in (22) is not necessary for the general framework and computational procedure to apply. The four parameters are $\mu_D(g,1,1)$, $\alpha(g,2,1)$, $\mu_D(g,2,1)$, and $\mu_D(g,2,2)$. The reader should note that $\alpha(g,2,2)$ is not among the list of parameters since it is determined by (6), $\alpha(g,2,2) = 1 - \alpha(g,2,1)$.

Fig. 6 is a plot of the pdf (22) for $\kappa^2 = 1, 2, 3, 4$ and a mean of one. Here, we see that all the pdf's in this family go through the origin. To the eye, the shape appears similar to the Erlang-2 pdf but it is much heavier on the tail. Moreover, it has a coefficient of variation that can be greater than unity, in contrast to that for the Erlang-2, which must be less than unity. SOHYP pdf's with more than two phases stay even closer to the origin as the abscissa increases from zero (because a SOHYP pdf with N phases $(N \geq 2)$ will go through the origin, as will its first $N-2$ derivatives). This behavior is similar to that of the Erlang pdf with N phases.

IV. Statement of Example Problem

This example considers single call platforms, handoffs with cutoff priority, mixed platform types, and SOHYP mobility characteristics.

- The system has G types of mobile platforms, indexed by $g = 1, 2, \cdots, G$. Each platform can support at most one call at a time. Platform mobilities are characterized by random variables $T_D(g), (g = 1, 2, \cdots G)$, each having a SOHYP distribution but with generally different parameters.
- The number of *noncommunicating g-type platforms* in any cell is denoted by $v(g, 0)$. It is assumed that $v(g, 0)$ is much larger than the total number of calls

that a cell can accommodate. In other words, an infinite population model is assumed.

- The new-call origination rate for a noncommunicating platform g-type platform is denoted $\Lambda(g)$. The total new-call origination rate for g-type calls is denoted by $\Lambda_n(g)$ and is expressed as $\Lambda_n(g) = \Lambda(g)v(g,0)$.
- *Channel limit*: Each gateway (or cell) can accommodate C calls.
- *Platform quotas*: Each gateway can accommodate $J(g)$ g-type calls simultaneously, where $J(g) \leq C$.
- *Cutoff priority*: At each gateway C_h channels are reserved for handoff calls. New calls will be blocked if the number of channels in use is greater than $C - C_h$, while handoff attempts will fail only if the number of channels in use is equal to C.
- The *unencumbered session time* of a g-type call is an NED random variable $T(g)$ with mean $\bar{T}(g) = 1/\mu(g)$. Note that we wish to emphasize that for convenience, we have taken the unencumbered session time to be NED. However, this variate too can be considered to be SOHYP distributed. The state space would have to be expanded to accommodate this. The approach would be completely analogous to that used for *dwell time* characterization in the current context. The use of the NED for session times has been common in teletraffic theory. However, since much less is known about dwell-time distributions, we focus attention on this aspect.
- The problem is to calculate performance measures including blocking probability, handoff failure probability, forced termination probability, and handoff activity.

The analysis is similar to that used in [1] and [2]. The differences are in the definition of the state variables and in the equations that specify the state probability transition flows. What follows is the development of the state characterization, transition rate, and probability flow balance equation that determine the state probabilities.

V. State Description

Consider first a single cell. The state variables for the cell are given by v_{gik} $\{g = 1, 2, \cdots, G, i = 1, 2, \cdots, N(g), k = 1, 2, \cdots, M(g,i)\}$, in which the state variable v_{gik} represents the number of platforms of type g that are in phase i and stage k. The state of a cell is a sequence of nonnegative integers, which can be conveniently written as G n-tuples. Specifically, a *cell state* is given by the matrix shown at the bottom of the page. It is convenient to order the states using the index $s = 0, 1, 2, \cdots, s_{\max}$. The state variables can then be expressed as functions of $s, g, i,$ and k. That is, $v(s,g,i,k)$ represents the number of g-type platforms in phase i and stage k when the cell is in state s.

The overall system consists of many cells. The *system state* is the concatenation of the states of all cells in the region of service. Because of handoffs, cell-state transitions are coupled. So a rigorous analysis requires the consideration of all possible system states. Because of the overwhelming dimensions of this problem, we resort to the approach put forth in [1], [2], and [7]. Specifically, a single cell is isolated, and its interaction with its neighbors its represented by *averaged* handoff arrival rates that are related to *averaged* handoff departure rates. (For homogenous systems, these rates must be equal. Nonhomogenous systems can be analyzed similarly [1], [2].) The result is a system of nonlinear equations to be solved for the *cell-state probabilities*.

When a cell is in state s, a number of characteristics can be determined. The number of channels in use by g-type platforms is

$$j(s,g) = \sum_{i=1}^{N(g)} \sum_{k=1}^{M(g,i)} v(s,g,i,k). \tag{23}$$

The total number of channels in use when the cell is in state s is found by

$$j(s) = \sum_{g=1}^{G} j(s,g). \tag{24}$$

A sequence of integers is a permissible state if all constraints are satisfied. For this framework, the channel limit (C) requires $j(s) \leq C$, and platform quotas $[J(g)]$ require $j(s,g) \leq J(g)$ for $g = 1, 2, \cdots, G$.

VI. Driving Processes and State Transitions

For this model, five driving processes can be identified. They are $\{n\}$, the generation of new calls; $\{c\}$, the completion of calls; $\{h\}$, the arrival of communicating platforms at the cell of interest; $\{d\}$, the departure of communicating calls from the cell of interest; and $\{\phi\}$, the transition between dwell-time phases. Since the model considers multiple platform types, the above processes are all multidimensional.

$$\begin{array}{ccccccccccccc}
v_{111} & v_{112} & \cdots & v_{11M(1,1)}, & v_{121} & v_{122} & \cdots & v_{12M(1,2)}, & \cdots, & v_{1N(1)1} & v_{1N(1)2} & \cdots & v_{1N(1)M(1,N(1))} \\
v_{211} & v_{212} & \cdots & v_{21M(2,1)}, & v_{221} & v_{222} & \cdots & v_{22M(2,2)}, & \cdots, & v_{2N(2)1} & v_{2N(2)2} & \cdots & v_{2N(2)M(2,N(2))} \\
\vdots & & & & & & & & & & & & \vdots \\
v_{g11} & v_{g12} & \cdots & v_{g1M(g,1)}, & v_{g21} & v_{g22} & \cdots & v_{g2M(g,2)}, & \cdots, & v_{gN(2)1} & v_{gN(2)2} & \cdots & v_{gN(g)M(g,N(g))} \\
\vdots & & & & & & & & & & & & \vdots \\
v_{G11} & v_{G12} & \cdots & v_{G1M(G,1)}, & v_{G21} & v_{G22} & \cdots & v_{G2M(G,2)}, & \cdots, & v_{GN(G)1} & v_{GN(G)2} & \cdots & v_{GN(G)M(G,N(G))}.
\end{array}$$

To use a multidimensional birth-death formulation, Markovian assumptions about the driving processes are involved. The new call-arrival process is assumed to follow a Poisson point process with state-dependent means. Call session time has been assumed to be NED distributed, so the call-completion process has the required memoryless property. The dwell time, however, has the SOHYP pdf, which itself does not have the memoryless property. However, by using the state description outlined in the previous section, the dwell time is decomposed into its phases and stages. Each of these is an NED, so the memoryless property can be used [29]. The handoff arrival process for each platform type is determined by the corresponding departure process. In considering the overall *system states* [1], [2], these are (system) state-dependent Poisson processes. In focusing on an individual cell, however, each is represented as a Poisson process having a parameter determined by the decoupling assumption of $\{h\}$ and $\{d\}$, as described in [1] and [2]. In comparison with dwell times that are NED, the cost of this more appropriate model requires an increase in the size (dimension and number of states) of the state space and generally longer computation times.

It remains to specify all of the state transitions. For every state, the possible predecessor states must be identified. A predecessor state is any state that could have immediately given rise to the current state under each of the driving processes described above. Also, the state probability transition flows must be found. Then the flow-balance equations can be determined and the state probabilities can be calculated [1], [2], [29].

In the paragraphs that follow, three dummy indexes z_1, z_2, and z_3 are used for convenience as follows: $z_1 = 1, 2, 3, \cdots, G$; $z_2 = 1, 2, 3, \cdots, N(z_1)$; and $z_3 = 1, 2, 3, \cdots, M(z_1, z_2)$. Recall that G is the number of platform types, $N(z_1)$ is the number of phases of dwell time for a platform of type z_1, and $M(z_1, z_2)$ is the number of possible stages for a platform of type z_1 in phase z_2.

A. New-Call Arrivals

A transition into state s from state x_n due to a new-call arrival on a g-type platform in phase i, stage k will cause the state variable $v(x_n, g, i, k)$ to be increased by one. Also, a new call can only be served if the total number of channels in use is less than $C - C_h$. Therefore, a permissible state x_n is a predecessor of state s for new-call arrivals on g-type platforms if $j(x_n) < C - C_h$, $j(x_n) < J(g)$, and the state variables are related by

$$\begin{aligned} v(x_n, g, i, k) &= v(s, g, i, k) - 1 \\ v(x_n, z_1, z_2, z_3) &= v(s, z_1, z_2, z_3) \quad z_1 \neq g \\ v(x_n, z_1, z_2, z_3) &= v(s, z_1, z_2, z_3) \quad z_2 \neq i \\ v(x_n, z_1, z_2, z_3) &= v(s, z_1, z_2, z_3) \quad z_3 \neq k. \end{aligned} \tag{25}$$

The probability that a new call will arrive at a g-type platform while the platform is in phase i and stage k is given by

$$\rho_n(g, i, k) = \frac{\alpha(g, i, k)/\mu_D(g, i, k)}{\bar{T}_D(g)}, \; k = 1, 2, \cdots, M(g, i). \tag{26}$$

The new-call arrival rate for calls on g-type platforms in phase i and stage k of dwell time can be expressed as

$$\Lambda_n(g, i, k) = \rho_n(g, i, k) \cdot \Lambda_n(g). \tag{27}$$

Last, the transition rate into state s from state x_n due to new-call arrivals is

$$\gamma_n(s, x_n) = \Lambda_n(g, i, k). \tag{28}$$

B. Call Completions

A transition into state s due to a call completion on a g-type platform in stage k of phase i when the cell is in state x_c causes the state variable $v(x_c, g, i, k)$ to be decreased by one. Therefore, a permissible state x_c is a predecessor of state s for call completion on g-type platforms in stage k of phase i if the state variables related by

$$\begin{aligned} v(x_c, g, i, k) &= v(s, g, i, k) + 1 \\ v(x_c, z_1, z_2, z_3) &= v(s, z_1, z_2, z_3) \quad z_1 \neq g \\ v(x_c, z_1, z_2, z_3) &= v(s, z_1, z_2, z_3) \quad z_2 \neq i \\ v(x_c, z_1, z_2, z_3) &= v(s, z_1, z_2, z_3) \quad z_3 \neq k. \end{aligned} \tag{29}$$

The corresponding transition rate is given by

$$\gamma_c(s, x_c) = \mu(g) \cdot v(x_c, g, i, k). \tag{30}$$

C. Handoff Arrivals

When a g-type platform enters a cell from a neighboring cell, it will enter in its *first phase* of dwell time. Therefore, a transition into state s from state x_h due to a handoff arrival on a g-type platform will cause the state variable $v(x_h, g, 1, k)$ to be incremented by one. Since handoff calls have access to all C channels in the target cell, a permissible state x_h is a predecessor of state s for handoff arrivals on g-type platforms in phase i and stage k if $j(x_h) < C$, $j(x_h) < J(g)$, and the state variables are related by

$$\begin{aligned} v(x_h, g, 1, k) &= v(s, g, 1, k) - 1 \\ v(x_h, z_1, z_2, z_3) &= v(s, z_1, z_2, z_3) \quad z_1 \neq g \\ v(x_h, z_1, z_2, z_3) &= v(s, z_1, z_2, z_3) \quad z_2 \neq i \\ v(x_h, z_1, z_2, z_3) &= v(s, z_1, z_2, z_3) \quad z_3 \neq k. \end{aligned} \tag{31}$$

When the platform enters the target cell, it begins its first phase and chooses a stage k $[k = 1, 2, \cdots, M(g, 1)]$ with probability $\alpha(g, 1, k)$. Let Λ_h be the overall average handoff arrival rate and F_g be the fraction of handoff arrivals that occur on g-type platforms. The rate of handoff arrivals of g-type platforms in phase one and stage k is given by

$$\Lambda_h(g, k) = \alpha(g, 1, k) \cdot \Lambda_h \cdot F_g \tag{32}$$

in which $\alpha(g, 1, k)$ is defined in (5). For now, the parameters Λ_h and F_g are assumed to be known, but they are actually functions of the state probabilities. Their values are determined in the iterative solution described later. The transition flow is given by

$$\gamma_h(s, x_h) = \Lambda_h(g, k). \tag{33}$$

D. Handoff Departures

A handoff departure of a g-type platform occurs when the platform completes its final phase $[i = N(g)]$ of dwell time. Therefore, a transition into state s due to a handoff departure of a g-type platform in stage k of its last $[i = N(g)]$ phase when the cell is in state x_d will cause the state variable $v(x_d, g, N(g), k)$ to be decreased by one. Thus, a permissible state x_d is a predecessor state of s for handoff departures of g-type platforms in stage k of phase $N(g)$ if the state variables are related by

$$\begin{aligned} v(x_d, g, N(g), k) &= v(s, g, N(g), k) - 1 \\ v(x_d, z_1, z_2, z_3) &= v(s, z_1, z_2, z_3) \quad z_1 \neq g \\ v(x_d, z_1, z_2, z_3) &= v(s, z_1, z_2, z_3) \quad z_2 \neq N(g) \\ v(x_d, z_1, z_2, z_3) &= v(s, z_1, z_2, z_3) \quad z_3 \neq k. \end{aligned} \tag{34}$$

The corresponding transition flow is given by

$$\gamma_d(s, x_d) = \mu_D(g, N(g), k) \cdot v(x_d, g, N(g), k). \tag{35}$$

E. Dwell-Time Phase Transitions

A transition into state s from state x_ϕ occurs when a platform, which is in phase i $[1 \leq i < N(g)]$ and stage k, completes its current dwell-time phase (i.e., stage k of phase i is completed). After completing phase i, the platform begins phase $i+1$. Therefore, the phase completion causes two state variables to change simultaneously. The state variable $v(x_\phi, g, i, k)$ will be decreased by one, and the state variable $v(x_\phi, g, i+1, k)$ will be increased by one. We limit the discussion of phase transitions to $1 \leq i < N(g)$ since a completion of phase $N(g)$ corresponds to a handoff departure and has already been considered. Thus, a permissible state x_ϕ is a predecessor state of s for dwell-time phase transitions of g-type platforms in phase i and stage k if the state variables are related by

$$\begin{aligned} v(x_\phi, g, i+1, k) &= v(s, g, i+1, k) - 1 \\ v(x_\phi, g, i, k) &= v(s, g, i, k) + 1 \\ v(x_\phi, z_1, z_2, z_3) &= v(s, z_1, z_2, z_3) \quad z_1 \neq g \\ v(x_\phi, z_1, z_2, z_3) &= v(s, z_1, z_2, z_3) \quad z_2 \neq i \end{aligned} \tag{36}$$

where $g = 1, 2, \cdots, G$, $i = 1, 2, \cdots, N(g) - 1$, and $k = 1, 2, \cdots, M(g, i)$.

For a g-type platform, the total rate $r_\phi(x_\phi, g, i)$, at which phase i (where $(1 \leq i < N(g))$ completions occur when the cell is in state x_ϕ, is given by

$$r_\phi(x_\phi, g, i) = \sum_{k=1}^{M(g,i)} \mu_D(g, i, k) \cdot v(x_\phi, g, i, k). \tag{37}$$

When a platform of type g completes phase i and enters phase $i+1$, it will choose stage k with probability $\alpha(g, i+1, k)$. Thus, the corresponding transition flow from state x_ϕ to state s is given by

$$\gamma_\phi(s, x_\phi) = \alpha(g, i+1, k) \cdot r_\phi(x_\phi, g, i). \tag{38}$$

VII. Flow-Balance Equations

The total transition flow into a state s from any permissible state x is the sum of the component flows due to the driving processes. This is expressed by the following:

$$\begin{aligned} q(s, x) = &\gamma_n(s, x) + \gamma_c(s, x) + \gamma_h(s, x) \\ &+ \gamma_d(s, x) + \gamma_\phi(s, x) \end{aligned} \tag{39}$$

where $q(s, x)$ is the total flow into state s from state x and $s \neq x$. Flow into a state is assigned a positive value, and flow out of a state is assigned negative values. The total flow out of state s is therefore written as

$$q(s, s) = -\sum_{\substack{n=0 \\ n \neq s}}^{S_{\max}} q(n, s). \tag{40}$$

When the system is in statistical equilibrium, the total flow into a state is equal to the total flow out of the state. The balance equations can be expressed as

$$\begin{aligned} &\sum_{j=0}^{S_{\max}} q(i, j) p(j) = 0 \quad i = 0, 1, 2, \cdots, s_{\max} - 1 \\ &\sum_{j=0}^{s_{\max}} p(j). \end{aligned} \tag{41}$$

The above are a set of $s_{\max} - 1$ simultaneous equations, which can be solved for the unknown state probabilities $p(j)$.

Previously, we assumed the parameters Λ_h (the average handoff arrival rate) and F_g (the fraction of handoffs that are g-type) where given. These are actually functions of the driving processes and must be determined from the processes themselves. The iterative approach described in [2] is used. We denote $\Delta_h(g, i)$ as the average handoff departure rate of g-type platforms in phase i. This is given by

$$\Delta_h(g, i) = \sum_{s=0}^{s_{\max}} \sum_{k=1}^{M(g,i)} v(s, g, i, k) \cdot \mu_D(g, i, k) \cdot p(s). \tag{42}$$

The average handoff departure rate of g-type platforms is then found by

$$\Delta_h(g) = \sum_{i=1}^{N(g)} \Delta_h(g, i) \tag{43}$$

and the total average departure rate is

$$\Delta_h = \sum_{g=1}^{G} \Delta_h(g). \tag{44}$$

The fraction of handoff departures that occur on g-type platforms is denoted F'_g and is given by

$$F'_g = \frac{\Delta_h(g)}{\Delta_h} \quad g = 1, 2, \cdots, G. \tag{45}$$

A handoff departure of a g-type platform from a cell causes a handoff arrival of the same type in another cell. Then, for a homogeneous system in equilibrium, the average handoff departure and arrival rates and the fraction of g-type arrivals and departures must be equal. This is expressed in the following:

$$F_g = F'_g \quad \text{and} \quad \Lambda_h = \Delta_h. \tag{46}$$

VIII. Computational Procedure

As stated earlier, the quantities F_g, Λ_h, and Δ_h, which appear in the determination of the transition flows $[q(i,j)s]$ in the flow-balance equations, depend on the unknown state probabilities $p(s)(s = 0, 1, 2, \cdots, s_{\max})$. Consequently, the flow-balance equations are actually a set of simultaneous nonlinear equations. A solution for the state probabilities $p(s)$, as well as Λ_h and Δ_h, can be obtained using an iterative approach [2]. For completeness of the present discussion, a brief outline of the solution procedure follows.

We define two functions $Q_1(\Lambda_h)$ and $Q_2(\Lambda_h)$. Q_1 is a vector function that takes Λ_h as its argument and returns all the state probabilities $p(s)$, fractions of g-type handoff departures F'_g, and the overall average handoff departure rate Δ_h. Q_2 is a scalar function of Λ_h. For a given Λ_h the function calls $Q_1(\Lambda_h)$ and returns the difference $\Lambda_h - \Delta_h$.

The function Q_1 is implemented in the following steps.

Step 1) Given Λ_h, begin with guesses or previous values for F_g. Solve the flow-balance equations for the state probabilities. We used a modified Gauss–Seidel algorithm to solve for the state probabilities; other methods for solving systems of linear equations can be used.

Step 2) Using the solution $[p(s)]$, determine the new fractions of g-type platform departures F'_g and compare with the previous values. If the relative error in any of the state probabilities $p(s)$ or fractions F_g exceeds some value (10^{-4} for accuracy of three significant figures), repeat Step 1) using the latest values for F_g. Otherwise, for the given Λ_h, and solution $p(s)$, determine the handoff departure rate Δ_h according to the formulas in the previous section. Return the latest values.

The complete solution is obtained by finding the root of $Q_2(\Lambda_h) = \Lambda_h - \Delta_h = 0$. For this purpose, we used a bisection algorithm. When the root of Q_2 is found, the average handoff arrival and departure rates will be equal, as required for a homogeneous system.

We point out that systems with SOHYP distributed dwell times will tend to have a larger state space (compared to NED dwell times) since several phases and stages are available for each platform type. The effect is that the computation time can be longer for the SOHYP system. To aid in the efficient computation of state probabilities, a good (close to the true value) initial guess of Λ_h is useful to reduce the number of iterations needed to obtain a solution. The relationship between handoff arrival rate and new-call arrival rate is discussed in [5]. If we consider that the new-call blocking probability and handoff failure probability are small, then using the results of [5], we obtain the following approximate expression for the handoff arrival rate of g-type calls:

$$\Lambda_h(g) = \Lambda_n(g) \cdot \frac{\bar{T}(g)}{\bar{T}_D(g)}. \tag{47}$$

The overall handoff rate is simply

$$\Lambda_h = \sum_{g=1}^{G} \Lambda_h(g) = \sum_{g=1}^{G} \Lambda_n(g) \cdot \frac{\bar{T}(g)}{\bar{T}_D(g)}. \tag{48}$$

Equation (48) can be used as the initial guess in the procedure described above.

IX. Performance Measures

Once the state transition flows and state probabilities are found, various performance measures that are functions of the state probabilities can be calculated.

A. Carried Traffic

The carried traffic per cell for each platform type is the average number of channels occupied by the calls from the given platform type. The carried traffic for g-type platforms is

$$A_c(g) = \sum_{s=0}^{s_{\max}} j(s,g) \cdot p(s). \tag{49}$$

The total carried traffic for all platform types, i.e., the total carried traffic per cell, is

$$A_c = \sum_{g=1}^{G} A_c(g). \tag{50}$$

B. Blocking Probability

The blocking probability for a new call on a g-type platform is defined as the average fraction of new calls that arrive on a g-type platform but are denied access to a channel. A new call on a g-type platform will be blocked if a) there are no channels available to serve the call or b) the number of g-type calls in progress is at the quota level $J(g)$. We define the following disjoint sets of states:

$$\begin{aligned} B_0 &= \{s : C - C_h \le j(s) \le C\} \\ B_g &= \{s : j(s) < C - C_h, j(s,g) = J(g)\} \end{aligned} \tag{51}$$

where $g = 1, 2, \cdots, G$. The blocking probability for a g-type call is then given by

$$P_B(g) = \sum_{s \in B_0} p(s) + \sum_{s \in B_g} p(s). \tag{52}$$

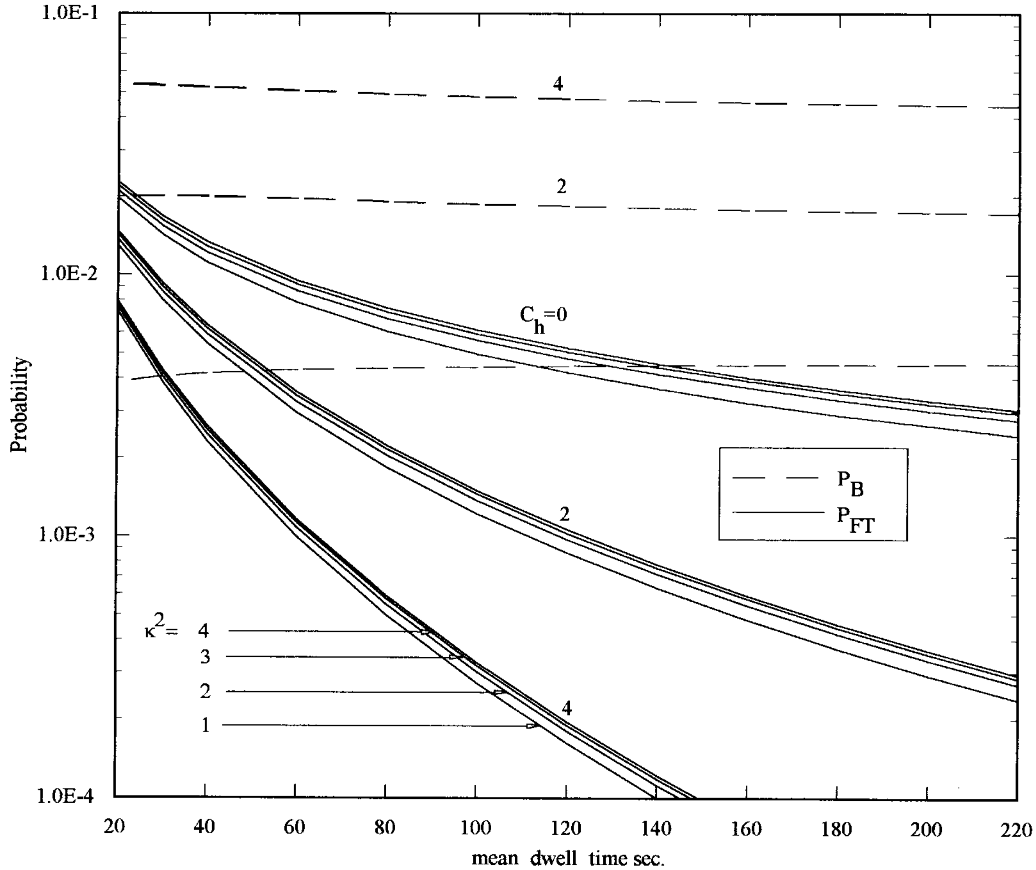

Fig. 7. Blocking and forced termination probabilities depend on dwell-time mean and variance. Dwell times are SOHYP distributed. $C = 20$, $C_h = 0, 2, 4$, $G = 1$, $N(1) = 2$, $M(1,1) = 1$, $M(1,2) = 2$, $v(1,0) = 400$, and $\Lambda(1) = 2.75$ E-04.

C. Handoff Failure Probability

The handoff failure probability for g-type calls is defined as the average fraction of g-type handoff attempts that are denied a channel. Handoff attempts have access to all C channels in a cell but may still be subject to channel quota constraints $[J(g)]$. Therefore, we have the following disjoint sets of states, for which handoff attempts will fail:

$$H_0 = \{s : j(s) = C\}$$
$$H_g = \{s : j(s) < C, j(s,g) = J(g)\}. \tag{53}$$

The handoff failure probability for a g-type handoff can be written as

$$P_H(g) = \sum_{s \in H_0} p(s) + \sum_{s \in H_g} p(s). \tag{54}$$

D. Forced Termination Probability

Forced termination probability for a g-type platform is denoted as $P_{\mathrm{FT}}(g)$. It is defined as the probability that a g-type call that is not blocked is interrupted due to a handoff failure during its lifetime. A *communicating* g-type platform in phase i $[i = 1, 2, \cdots, N(g)]$ must complete its *remaining* dwell-time phases to require a handoff. There are $N(g)-i+1$ remaining when a platform is in phase i. Recall that all phases are hyperexponentially distributed, and phase i has $M(g,i)$ stages. A platform selects a stage k for its ith phase from the $M(g,i)$ stages available with probability $\alpha(g,i,k)$. Let $\pi_i(g \mid k)$ be the conditional probability that a communicating platform in phase i completes the current phase before its call is completed, given that it is in stage k

$$\pi_i(g \mid k) = \frac{\alpha(g,i,k) \cdot \mu_D(g,i,k)}{\mu_D(g,i,k) + \mu(g)}. \tag{55}$$

We now define $\pi_i(g)$ to be the probability that a communicating g-type platform completes phase i of dwell time before its call is completed. That is, the platform completes its current stage of phase i

$$\pi_i(g) = \sum_{k=1}^{M(g,i)} \frac{\alpha(g,i,k) \cdot \mu_D(g,i,k)}{\mu_D(g,i,k) + \mu(g)}. \tag{56}$$

For a call being served on a g-type platform in phase i to generate a handoff attempt, $N(g) - i + 1$ dwell-time phases must be completed before the call completes. The probability that such a call will require a handoff is

$$b(g,i) = \prod_{n=i}^{N(g)} \pi_n(g). \tag{57}$$

Note that the right side of (57) is a product because each phase is independent of the others.

When a new call begins service, it arrives on a g-type platform in phase i and stage k of the platform's dwell

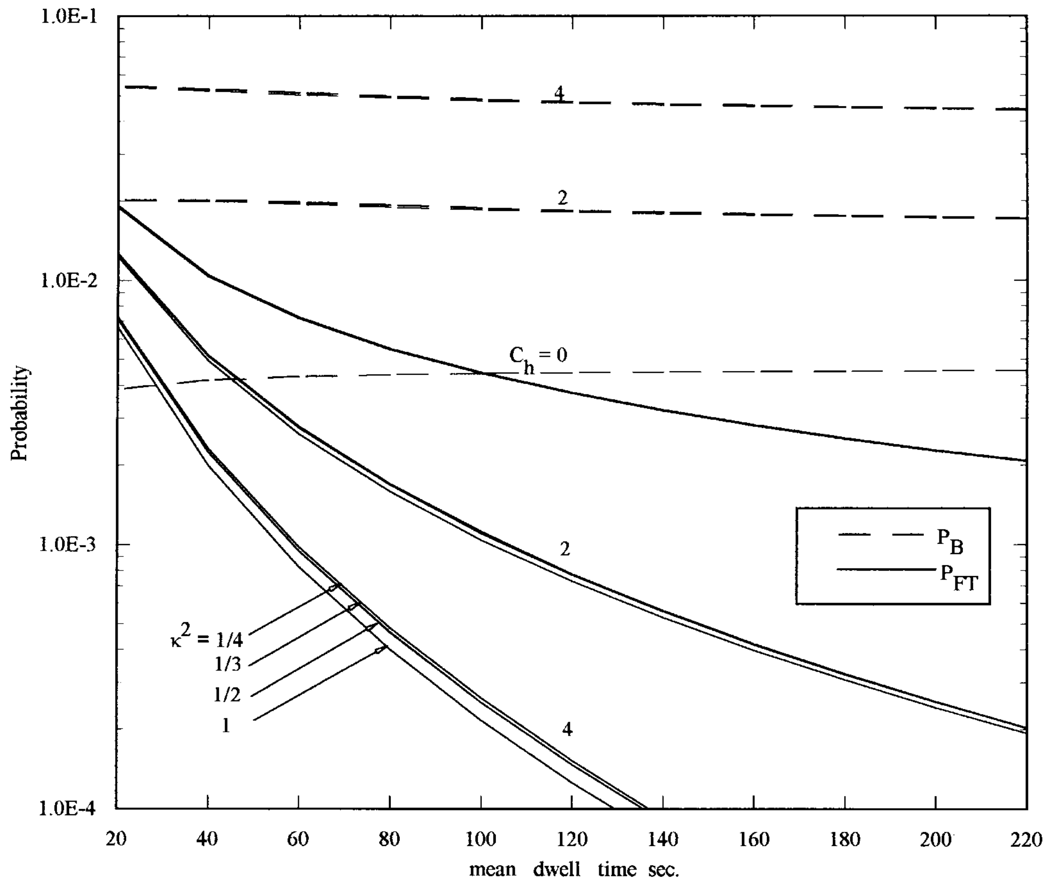

Fig. 8. Blocking and forced termination probabilities depend on dwell-time mean and variance. Dwell times are Erlang distributed. $C = 20$, $C_h = 0, 2, 4$, $G = 1$, $N(1) = 1, 2, 3, 4$, $v(1, 0) = 400$, $\bar{T} = 100$ s, and $\Lambda(1) = 2.75$ E-04.

time with a probability given by (27). The fraction of new calls that arrive on g-type platforms in phase i is given by

$$\rho_n(g, i) = \frac{\bar{T}_D(g, i)}{\bar{T}_D(g)} = \frac{\sum_{k=1}^{M(g,i)} \alpha(g, i, k)/\mu_D(g, i, k)}{\bar{T}_D(g)} \tag{58}$$

We can now write the probability that a new call on a g-type platform requires a handoff. This is given by

$$b(g) = \sum_{i=1}^{N(g)} \rho_n(g, i) \cdot b(g, i). \tag{59}$$

A call that is successfully handed off enters its target cell in the first phase of dwell time. Thus, the probability that a call onboard a g-type platform that has been handed off requires another handoff is $b(g, 1)$.

The probability that a call is forced to terminate on its kth handoff attempt is the probability of $k - 1$ successful handoffs followed by a handoff failure on the kth attempt. This is given by

$$Y(g, k) = b(g) \cdot P_H(g) \cdot \{b(g, 1) \cdot [1 - P_H(g)]\}^{k-1}. \tag{60}$$

The overall forced termination probability is

$$P_{\text{FT}}(g) = \sum_{k=1}^{\infty} Y(g, k). \tag{61}$$

We recognize the above as a geometric series and write the sum closed form as

$$P_{\text{FT}}(g) = \frac{b(g) \cdot P_H(g)}{[1 - \Psi(g)]}$$

where

$$\Psi(g) \equiv b(g, 1) \cdot [1 - P_H(g)]. \tag{62}$$

E. Handoff Activity Factor

The handoff activity factor $\eta(g)$ is defined to be the expected number of handoff attempts for nonblocked calls on g-type platforms. The derivation of the expression for $\eta(g)$ and the expression itself are identical to those given in [2]. The result is shown below

$$\eta(g) = \frac{b(g)}{[1 - \Psi(g)]} \tag{63}$$

where $b(g)$ is defined in (59) and $\Psi(g)$ is defined in (62).

X. Discussion of Results

Numerical results were generated using the method described here. Fig. 7 is a plot of blocking probability and forced termination probability versus mean dwell time. The system considered has a single platform type $G = 1$ with two phases, $N(1) = 2$. The first phase is NED,

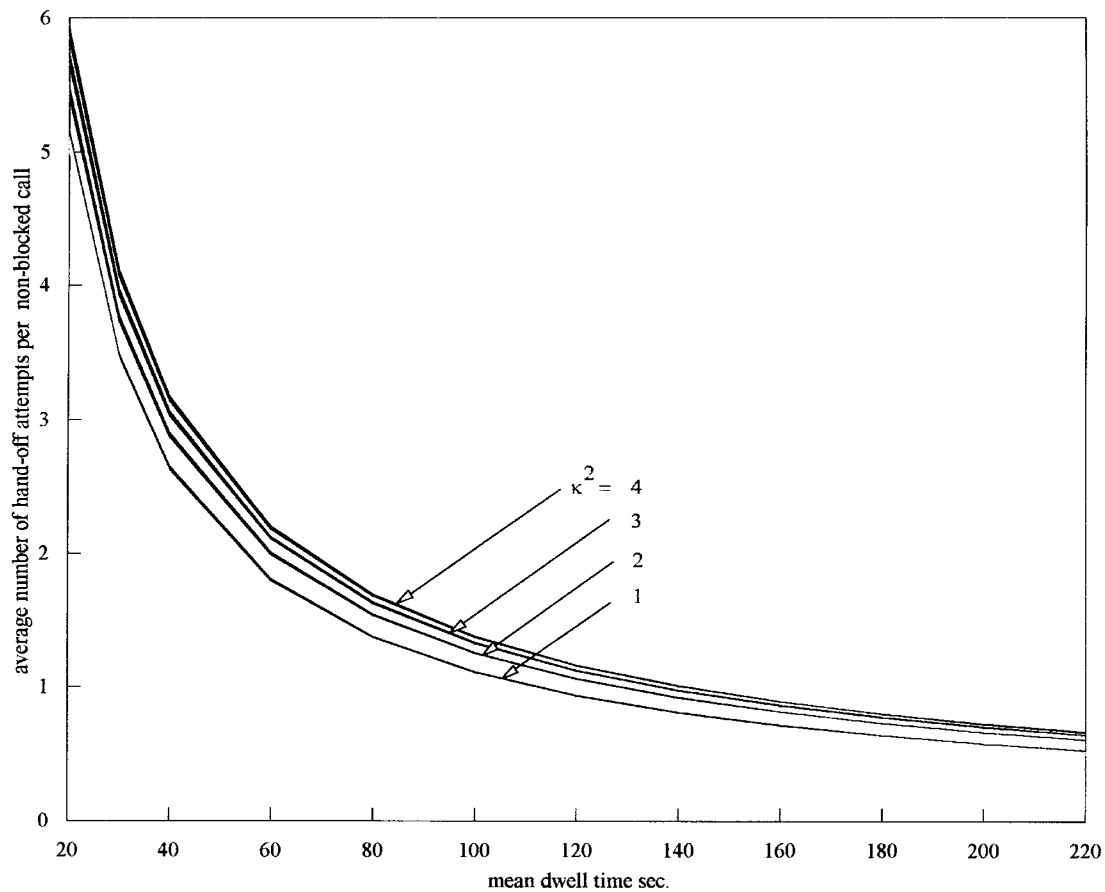

Fig. 9. Handoff activity depends on dwell-time mean and variance. Dwell times are SOHYP distributed. $C = 20$, $C_h = 0, 2, 4$, $G = 1$, $N(1) = 2$, $M(1,1) = 1$, $M(1,2) = 2$, $v(1,0) = 400$, and $\Lambda(1) = 2.75$ E-04.

and the second phase is hyperexponential with two stages ($M(1,1) = 1$ and $M(1,2) = 2$). The mean unencumbered session time is assumed to be 100 s, and the new-call arrival rate per platform $[\Lambda(1)]$ is constant at 2.75E-04 calls/s (approximately one call per hour per platform). Cells have 20 channels each ($C = 20$), and the number of platforms in each cell was set at 400 ($v(1,0) = 400$). No channel quotas are considered. The effect of reserving channels for handoffs is also shown ($C_h = 0, 2, 4$). Fig. 7 shows the effect of mean dwell time and variance on blocking and forced termination probabilities.

We see that as the coefficient of variation increases, the forced termination probability increases slightly for each C_h. This is expected, since a large coefficient of variation κ corresponds to a large spread of dwell times around the mean, making it more likely that some calls require several handoffs. Also shown in the figure is the decrease in forced termination as the dwell time increases. This is because calls on a platform with a large mean dwell time relative to the mean session time will require fewer handoffs. The blocking probability is insensitive to both mean dwell time and coefficient of variation.

Fig. 8 is again a plot of blocking and forced termination probabilities. For this figure, however, the platform dwell time is distributed according to the Erlang pdf. The results shown in Fig. 8 were obtained using the method in [2]. The parameters of the system are identical to those in Fig. 7, except that the number of phases varies from one to four $[N(g) = 1, 2, 3, 4]$, which yields squared coefficients of variations $\kappa^2 = 1, 1/2, 1/3, 1/4$. For this system, the blocking probability is found to be insensitive to mean dwell time and variance. The forced termination probabilities increase slightly as the coefficient of variation decreases.

The handoff activity for the cellular system with SOHYP distributed dwell times is shown in Fig. 9. The system parameters are the same for those in Fig. 7. We see from the figure that increasing the dwell-time coefficient of variation (while keeping the mean fixed) causes an increase in the average number of handoff attempts per nonblocked call. It is also seen that handoff activity decreases as the mean dwell time increases.

Figs. 7 and 8 show that the use of negative exponential variates for dwell time produces essentially the same blocking probabilities as more elaborate models. Also from the figures, we see that the negative exponential ($\kappa^2 = 1$ in Fig. 8) gives the minimum forced termination probability, and the effect of varying κ^2 on forced termination probability is small. Since the NED requires the fewest states, in this framework, it can be used as a dwell-time model to obtain results quickly when investigating the impact of other issues on performance—but the forced termination performance may be *slightly* optimistic.

ACKNOWLEDGMENT

The authors wish to gratefully acknowledge additional support from Hughes Network Systems.

REFERENCES

[1] S. S. Rappaport, "The multiple hand-off problem in high capacity cellular communication systems," *IEEE Trans. Veh. Technol.*, vol. 40, no. 3, pp. 546–557, 1991.

[2] ——, "Blocking, hand-off and traffic performance for cellular communications with mixed platforms," *Proc. Inst. Elect. Eng. 1*, vol. 140, no. 5, pp. 389–401, 1993.

[3] D. Hong and S. S. Rappaport, "Traffic model and performance analysis for cellular mobile radiotelephone systems with prioritized and nonprioritized hand-off procedures," *IEEE Trans. Veh. Technol.*, vol. VT-35, pp. 77–92, 1986.

[4] P. Orlik and S. S. Rappaport, "Traffic performance and mobility modeling of cellular communications with mixed platforms and highly variable mobilities," in *Proc. VTC'97*, May 1997, pp. 587–591.

[5] S. S. Rappaport and C. Purzynski, "Prioritized resource assignment for mobile cellular communication systems with mixed services and platform types," *IEEE Trans. Veh. Technol.*, vol. 45, pp. 443–457, 1996.

[6] S. S. Rappaport and L.-R. Hu, "Microcellular communication systems with hierarchical macrocell overlays: Traffic performance models and analysis," *Proc. IEEE*, vol. 82, pp. 1383–1397, Sept. 1994.

[7] S. S. Rappaport, "Models for call hand-off schemes in cellular communication networks," in *Third Generation Wireless Information Networks*, S. Nanda and D. J. Goodman, Eds. Boston, MA: Kluwer, 1992, pp. 163–185.

[8] R. Steele and M. Nofal, "Teletraffic performance of microcellular personal communication networks," *Proc. Inst. Elect. Eng.*, vol. 139, pt. I, no. 4, pp. 448–461, Aug. 1992.

[9] D. McMillan, "Traffic modeling and analysis for cellular mobile networks," in *Proc. Teletraffic and Data Traffic in a Period of Change (ITC-13)*, 1991, pp. 627–632.

[10] B. Jabbari, "Teletraffic aspects of evolving and next generation wireless communication networks," *IEEE Personal Commun.*, pp. 4–9, Dec. 1996.

[11] Y.-B. Lin, "Determining the user locations for personal communications services networks," *IEEE Trans. Veh. Technol.*, vol. 43, pp. 466–473, Aug. 1994.

[12] S. Tabbane, "An alternative strategy for location tracking," *IEEE J. Select. Areas Commun.*, vol. 13, pp. 880–892, June 1995.

[13] J. Z. Wang, "A fully distributed location registration strategy for universal personal communication systems," *IEEE J. Select. Areas Commun.*, vol. 11, pp. 850–860, Aug. 1993.

[14] M. Gudmundson, "Analysis of handover algorithms," in *Proc. IEEE VTC'91*, May 1991, pp. 537–542.

[15] O. Grimlund and M. Gudmundson, "Handoff strategies in microcellular systems," in *Proc. IEEE VTC'91*, May 1991, pp. 505–510.

[16] M. D. Austin and G. L. Stuber, "Velocity adaptive handoff algorithms for microcellular systems," *IEEE Trans. Veh. Technol.*, vol. 43, pp. 549–561, Aug. 1994.

[17] R. Guerin, "Channel occupancy time distribution in a cellular radio system," *IEEE Trans. Veh. Technol.*, vol. VT-36, pp. 89–99, Aug. 1987.

[18] ——, "Queueing-blocking system with two arrival streams and guard channels," *IEEE Trans. Commun.*, vol. 36, no. 2, pp. 153–163, 1988.

[19] T. P. Chu and S. S. Rappaport, "Overlapping coverage with reuse partitioning in cellular communication systems," *IEEE Trans. Veh. Technol.*, vol. 46, pp. 41–54, Feb. 1997.

[20] S. L. Su, J. Y. Chen, and J. H. Huang, "Performance analysis of soft handoff in CDMA cellular networks," *IEEE J. Select. Areas Commun.*, vol. 14, pp. 1762–1769, Dec. 1996.

[21] M. M. Zonoozi, P. Dassanayake, and M. Faulkner, "Mobility modeling and channel holding time distribution in cellular mobile communication systems," in *Proc. IEEE Globecom'95*, pp. 12–16.

[22] J. S. M. Ho and I. F. Akyildiz, "Mobile user location update and paging under delay constraints," *Wireless Networks*, vol. 1, pp. 413–425, 1995.

[23] C. Rose and R. Yates, "Location uncertainty in mobile networks: A theoretical framework," *IEEE Commun. Mag.*, vol. 35, pp. 94–101, Feb. 1997.

[24] D. Lam, D. C. Cox, and J. Widom, "Teletraffic modeling for personal communications services," *IEEE Commun. Mag.*, vol. 35, pp. 79–87, Feb. 1997.

[25] F. Khan and D. Zeghlache, "Effect of cell residence time distribution on the performance of cellular mobile networks," in *Proc. IEEE VTC*, May 1997, pp. 949–953.

[26] A. O. Allen, *Probability, Statistics, and Queueing Theory With Computer Science Applications*, 2nd ed. San Diego, CA: Academic, 1990.

[27] C. T. Chen, *System and Signal Analysis*. New York: Saunders College, 1989.

[28] A. Papoulis, *Probability, Random Variables, and Stochastic Processes*, 3rd ed. New York: McGraw-Hill, 1991.

[29] R. B. Cooper, *Introduction to Queuing Theory*, 2nd ed. New York: North-Holland, 1981.

Philip V. Orlik (Student Member, IEEE) was born in New York in 1972. He received the B.E. and M.E. degrees from the State University of New York at Stony Brook in 1994 and 1997, respectively. He currently is pursuing the Ph.D. degree in electrical engineering there.

He is a Research Assistant with the State University of New York at Stony Brook. His research interests include cellular communications, mobility modeling, performance analysis, and queueing theory.

Stephen S. Rappaport (Fellow, IEEE) received the B.E.E. degree from the Cooper Union, New York, in 1960, the M.S.E.E. degree from the University of Southern California, Los Angeles, in 1962, and the Ph.D. degree in electrical engineering from New York University, New York, in 1965.

He is Leading Professor of Electrical Engineering at the State University of New York at Stony Brook. His research has received substantial funding from the U.S. National Science Foundation and the U.S. Office of Naval Research. His experience includes Technical Staff positions with Hughes Aircraft Company and Bell Telephone Laboratories as well as consulting for industrial firms. In spring 1989, he was a Visiting Senior Research Scientist at Columbia University's Center for Telecommunications Research, New York. He has been on the editorial board of*Wireless Networks Journal*. He was a Guest Editor of *ACM-Baltzer WINET*.

From 1994 to 1996, Prof. Rappaport was Chairman of the IEEE Communications Society's Technical Committee on Personal Communications. He currently is Technical Program Vice-Chair of the IEEE 1998 International Conference on Universal Personal Communications. He has been on the Editorial Board of IEEE COMMUNICATIONS MAGAZINE and IEEE TRANSACTIONS ON COMMUNICATIONS. He is a member of the IEEE Communications Society and the Long Island Section. He has been a member of the IEEE Communications Society's Board of Governors, Nominations and Elections Board, Awards Board, Fellow Evaluation Committee, Communications Society Conference Board, Advisory Council, Technical Affairs Council, and Technical Program Committees for major conferences and workshops. He has been Chairman, Technical Committee on Data Communications Systems; National Chairman for Universities on the Member Activities Council; Chairman, Long Island Section Award Nominations Committee; First Vice-Chair, Long Island Section; Treasurer, Long Island Section; Chairman, Long Island Communications Society Chapter. He has been an Associate Editor for IEEE TRANSACTIONS ON COMMUNICATIONS and COMMUNICATIONS MAGAZINE. He was a Guest Editor of IEEE JOURNAL ON SELECTED AREAS IN COMMUNICATIONS. In 1995, he received the Mountbatten Premium from the Institute of Electrical Engineers (UK). He has been listed in *American Men & Women of Science*, *Who's Who in America*, *Who's Who In the East*, *Who's Who In Technology Today*, and *Who's Who in Science and Engineering*.